



Published in final edited form as:

Epilepsy Res. 2010 February ; 88(2-3): 208–214. doi:10.1016/j.epilepsyres.2009.11.011.

Children with New Onset Epilepsy Exhibit Diffusion Abnormalities in Cerebral White Matter in the Absence of Volumetric Differences

Elizabeth Hutchinson^{1,4,*}, Dalin Pulsipher², Kevin Dabbs³, Adan Myers y Gutierrez³, Raj Sheth³, Jana Jones³, Michael Seidenberg², Elizabeth Meyerand^{1,4}, and Bruce Hermann³

¹Neuroscience Training Program, University of Wisconsin7225 Medical Sciences Center, 1300 University Avenue, Madison, WI 53706

²Department of Psychology, Rosalind Franklin University of Medicine and Science 3333 Green Bay Rd, North Chicago, IL 60064

³Department of Neurology, University of Wisconsin School of Medicine and Public Health 600 Highland Ave, Madison, WI 53792

⁴Department of Medical Physics, University of WisconsinWisconsin Institutes for Medical Research, 1111 Highland Avenue, Room 1005 Madison, WI 53705

SUMMARY

The purpose of this investigation was to examine the diffusion properties of cerebral white matter in children with recent onset epilepsy (n=19) compared to healthy controls (n=11). Subjects underwent DTI with quantification of mean diffusion (MD), fractional anisotropy (FA), axial diffusivity (D_{ax}) and radial diffusivity (D_{rad}) for regions of interest including anterior and posterior corpus callosum, fornix, cingulum, and internal and external capsules. Quantitative volumetrics were also performed for the corpus callosum and its subregions (anterior, midbody and posterior) and total lobar white and gray matter for the frontal, parietal, temporal and occipital lobes. The results demonstrated no group differences in total lobar gray or white matter volumes or volume of the corpus callosum and its subregions, but did show reduced FA and increased D_{rad} in the posterior corpus callosum and cingulum. These results provide the earliest indication of microstructural abnormality in cerebral white matter among children with idiopathic epilepsies. This abnormality occurs in the context of normal volumetrics and suggests disruption in myelination processes.

Keywords

DTI; volumetrics; MRI; epilepsy

1. INTRODUCTION

Diffusion tensor imaging (DTI) studies have characterized abnormalities in the microstructural integrity of cerebral white matter in patients with chronic epilepsy including temporal lobe epilepsy (Duncan, 2008; Yogarajah et al., 2008; Yogarajah and Duncan, 2008) and other epilepsy syndromes such as juvenile myoclonic epilepsy (Deppe et al., 2008). Among patients

*Correspondence to: Elizabeth Hutchinson, ehutchinson@wisc.edu, Fax – (608) 265-9840.

Publisher's Disclaimer: This is a PDF file of an unedited manuscript that has been accepted for publication. As a service to our customers we are providing this early version of the manuscript. The manuscript will undergo copyediting, typesetting, and review of the resulting proof before it is published in its final citable form. Please note that during the production process errors may be discovered which could affect the content, and all legal disclaimers that apply to the journal pertain.

with temporal lobe epilepsy, DTI abnormalities have been reported in regions both near to as well as distant from the primary epileptic zone (Arfanakis et al., 2002; Concha et al., 2005; Concha et al., 2009; Gong et al., 2008; Gross et al., 2006; Kim et al., 2008; Lui et al., 2005; Thivard et al., 2005).

The early onset and long duration of commonly investigated epilepsy syndromes such as temporal lobe epilepsy raises the possibility that both neurodevelopmental and progressive processes may underlie the presence and distributed nature of these abnormalities. To address the neurodevelopmental contribution, investigation of children with a limited duration of epilepsy might prove helpful, but a remarkably limited number of studies have utilized DTI to understand the presence and course of white matter changes over time. Pediatric studies have focused primarily on children with localization-related and predominantly temporal lobe epilepsy. Findings include significantly reduced fractional anisotropy (FA) in the hippocampus contralateral as well as ipsilateral to side of seizure onset (Kimiwada et al., 2006); decreased anisotropy in white matter tracts (uncinate, arcuate, and inferior longitudinal fasciculi as well as corticospinal tract) both contralateral as well as ipsilateral to the side of seizure onset (Govindan et al., 2008), and increased diffusivity in temporal lobe and cingulate gyrus white matter but without significant differences in FA (Nilsson et al., 2008). Thus, even early in the course of epilepsy the microstructural integrity of cerebral white matter is affected.

The purpose here is to build upon these observations by examining diffusion properties in specific cerebral white matter tracts among children with recent onset and thereby very limited duration of epilepsy, thus representing the earliest investigation of these tissue properties in the natural course of childhood epilepsy. Our DTI studies were supplemented by examination of corpus callosum and lobar gray and white matter tissue volumes. White matter volumes were examined in order to determine whether abnormalities in diffusion properties occurred independently of cerebral white matter volume differences. Gray matter volumes were examined to address the possibility that diffusion abnormalities were a secondary consequence of gray matter degradation. While several white matter tracts were examined in this study, a specific focus was the corpus callosum where relatively direct comparisons could be made between DTI and volume measurements.

2. Methods

2.1 Subject groups

The participants were children 8-18 years of age including 19 patients with recent onset idiopathic epilepsy (average age \pm s.d. = 12.5 \pm 3.4 years; 8 female, 11 male) and 11 healthy controls (average age \pm s.d. = 13.8 \pm 3.4 years; 6 female, 5 male). In addition to age requirements, inclusion criteria for the patient group included a diagnosis of epilepsy within the past 12 months and no other developmental disabilities or neurological disorder. The patients met ILAE criteria for idiopathic epilepsy, meaning that there were no identifiable lesions or other abnormalities on clinical MRI nor neurological deficits on examination. The group was composed of 11 children with idiopathic generalized (average age \pm s.d. = 10.5 \pm 1.8 years; 4 female, 7 male) and 8 with localization related epilepsies (average age \pm s.d. = 15.2 \pm 3.2 years; 4 female, 4 male). Age was accounted for by all analysis methods and the distribution of syndromes within the patient group is given in table 1.

The following process was used to define the electroclinical syndromes. All children with epilepsy underwent a standard clinical EEG which was digitized and independently reviewed and coded by the project pediatric epileptologist for the following: 1) background rhythm, 2) presence/rate of diffuse slow waves, 3) presence, laterality and location of focal slow waves, 4) presence, laterality and location of epileptiform discharges, 5) presence of abnormalities activated by sleep, and 6) results of seizure onset if ictal recordings were obtained. This review

was conducted while blinded to all MRI, cognitive, and psychiatric data. This information was used with clinical characterization of seizures and history to define electroclinical syndromes in consensus conference.

Controls were first-degree cousins who were age and gender matched with no history of seizures, early initial precipitating injuries (e.g., febrile convulsions), no other developmental or neurological disease, or loss of consciousness greater than five minutes. Participants in both groups attended regular school. Further details regarding subject selection criteria are available in (Hermann et al., 2006). There were no significant differences between the epilepsy and control groups in age (12.6 vs. 13.6, $p=.43$), gender (53% male vs. 45% male, $p=.70$), or Full Scale IQ (96.6 vs. 97.1, $p=.89$).

2.2 Imaging parameters

Images were obtained on a 1.5 Tesla GE Signa MR scanner. Sequences acquired for each participant included: (i) T1-weighted, three-dimensional SPGR acquired with the following parameters: TE = 5ms, TR = 24ms, flip angle = 40deg, NEX = 1, slice thickness = 1.5 mm, slices = 124, plane = coronal, FOV = 20×20 cm², matrix = 256X256; (ii) proton density (PD) and (iii) T2-weighted images acquired with the following parameters: TE = 36ms (for PD) or 96 msec (for T2), TR = 3000 ms, NEX = 1, slice thickness = 3.0 mm, slices = 64, slice plane = coronal, FOV = 20×20 cm², matrix = 256X256; (iv) EPI DTI data series of one reference image ($b=0$ s/mm²) and 13 diffusion weighted images ($b=1000$ s/mm², non-colinear gradient orientations) with the following parameters: TE = 76.6 msec, TR = 4000 msec, NEX = 4, slice thickness = 4 mm and gap thickness = 4 mm, slices=15, slice plane = axial, FOV = 24×24 cm², matrix = 256 \times 256 (reconstructed).

2.3 Volumetric postacquisition processing

MRIs were processed using a semi-automated software package, i.e., Brain Research: Analysis of Images, Networks, and Systems (BRAINS2) (Andreasen et al., 1996; Harris et al., 1999). Neuroimaging analyses were conducted blinded to group status and both clinical and demographic characteristics of the subjects. The T1-weighted images were spatially normalized so that the anterior-posterior axis of the brain was realigned parallel to the anterior commissure - posterior commissure (ACPC) line, and the interhemispheric fissure was aligned on the other two axes. A six-point linear transformation was used to warp the standard Talairach atlas space onto the resampled image. Images from the three pulse sequences were then coregistered using a local adaptation of automated image registration software. Following alignment of the image sets, all images were resampled into 1 mm cubic voxels, following which an automated algorithm classified each voxel as gray matter, white matter, CSF, blood, or "other." Manual inspection and correction of the output of the neural network tracing was conducted. The brain images were then volume rendered using local utilities, producing tissue volumes for regions of interest within the brain. The six outer boundaries of the brain form a bounding box that along with the AC-PC line produces a volumetric grid based on the Talairach divisions. Each lobar volume measured is defined in this proportional coordinate system. Thus, all measurements are obtained in the image space of the subject without morphing the image to fit a standard brain atlas. Dependent measures were white and gray matter volumes of the left and right frontal, parietal, temporal and occipital lobes. All volumes were adjusted for age and total intracranial volume (ICV).

2.4 Corpus callosum guidelines

Manual trace of the corpus callosum began in the midsagittal plane. Using a previously established tracing protocol (Hermann et al., 2003b), three co-registered image sets were used simultaneously to delineate the corpus callosum. Boundary identification was based on a pre-manipulated trimodal image (a composite of the T1, T2, and PD images) as the primary image

set, with reference to the continuously segmented image, and a discretely segmented image in areas of poorly defined borders (such as the confluence of the fornix and the ventral callosum). Additionally, voxel signal intensities were used to separate white matter voxels from neighboring voxels of cerebral spinal fluid, blood vessel wall, and gray matter. In addition to the midsagittal slice, two additional slices extending laterally from the midsagittal view were traced. The anterior and posterior extreme of the corpus callosum trace were kept consistent when extending the trace to parasagittal slices. Although the lateral extent of the corpus callosum extends beyond the central five sagittal slices, these regions were excluded from the trace due to difficulty in boundary determination. In addition, a BRAINS2 script was applied to automatically partition the CC into seven regions defined by Witelson (Witelson, 1989). This technique used the inner convexity of the genu as a landmark in conjunction with the rostral-caudal axis length to subdivide the callosum. Witelson regions were then summed to create anterior (1-3), midbody (4-5), and posterior (6-7) regions (Hermann et al., 2003a). An interrater agreement (κ) of .99 was achieved. Dependent measures were the volumes of the total corpus callosum as well as the anterior, midbody and posterior regions of the corpus callosum. In order to account for head size volumetric differences, all callosal volumes were adjusted for age and total intracranial volume (ICV).

2.5 DTI postacquisition processing

Offline processing of the DTI datasets was completed using the diffusion II toolbox for SPM5 in Matlab. The reference and diffusion weighted images were first corrected for motion and field inhomogeneity artifacts by coregistration of the image volumes. Next, the diffusion tensor was calculated at each voxel and maps for the mean diffusion (MD), fractional anisotropy (FA), axial diffusivity (D_{ax}) and radial diffusivity (D_{rad}) were calculated for each subject.

In order to quantify diffusion indices of six specific white matter structures, the anterior and posterior corpus callosum, fornix, cingulum, internal capsule and external capsule, binary masks of regions of interest (ROIs) were created using FSL software (Smith et al., 2004) and according to anatomical landmarks on axial slices of the FA map. All ROI masks were bilateral. For the anterior and posterior corpus callosum a single axial slice was selected for which the structure was the most apparent and ROIs were constrained to the medial 13.5 mm of each structure for consistency with volumetric data. For the other white matter structures, all slices containing a given structure were included in creating the ROI mask. Initially, masks were coarsely drawn to include structure edges and surrounding gray matter, but to exclude all other white matter. Next, an FA threshold was applied to refine the rough masks to include only white matter voxels. This FA threshold was set at 0.5 for the corpus callosum regions and 0.45 for the other regions. For the anterior and posterior corpus callosum masks, the anterior and posterior edges were further eroded by two voxels in order to reduce partial volume effects near the structure edges. ROI masks were applied to DTI index maps to calculate mean values for each structure for each subject. The FA map for a representative subject is shown in figure 1 with the ROI masks overlaid. Analysis of covariance with age as a covariate was used to test for group differences after accounting for age effects.

3. Results

3.1 Lobar gray and white matter volumes

There were no significant differences between the epilepsy and control groups in age and ICV adjusted gray and white matter volumes. Specifically, there were no significant univariate effects for lobar frontal ($p=.94$), parietal ($p=.46$), temporal ($p=.56$), or occipital ($p=.98$) white matter volumes. There were also no significant univariate effects for lobar frontal ($p=.73$), parietal ($p=.38$), temporal ($p=.46$) or occipital ($p=.44$) gray matter volumes (see figure 2).

3.2 Corpus callosum volumes

There were no significant differences between the epilepsy and control groups in age and ICV corrected volumes of the total corpus callosum ($p=.69$) as well as the anterior ($p=.60$), midbody ($p=.98$), and posterior ($p=.15$) regions (see figure 3).

3.3 Diffusion indices

DTI indices of FA, MD, D_{ax} and D_{rad} were analyzed for the anterior and posterior corpus callosum, fornix, cingulum, internal capsule and external capsule and compared between epilepsy patients and controls. Analysis of covariance with age as a covariate showed a group difference of reduced FA for the posterior corpus callosum ($p=0.04$) and cingulum ($p=0.04$) in the epilepsy group. Additionally, there was an increase in MD for the posterior corpus callosum ($p=0.03$). There were no significant group differences for D_{ax} in any region. However, D_{rad} was significantly increased in the cingulum ($p=0.03$) and posterior corpus callosum ($p=.03$) (see figure 4).

When the epilepsy group was divided into localization related (LRE) and idiopathic generalized (IGE) groups, non-significant trends were observed to follow the findings of the pooled group for both the posterior corpus callosum and cingulum. Additionally, there was significantly increased MD and D_{rad} ($p=0.039$ and 0.043 respectively) in the fornix of the LRE group, but not the IGE group compared to controls (see supplemental table 1).

4. Discussion

The primary finding of this study is the presence of DTI abnormalities in the white matter of children with very recent onset idiopathic epilepsies compared to control children. These diffusion abnormalities occur in the context of comparable volumes of lobar gray and white matter in the frontal, parietal, temporal and occipital lobes. Volumetric analysis of the corpus callosum also shows no difference for the total corpus callosum as well as for the anterior, posterior or middle subregions in particular. Taken together, these findings imply an early vulnerability of the structural integrity of cerebral white matter in new-onset epilepsy to which DTI, but not volumetric analysis, is sensitive. Our results extend previous DTI investigations of children with epilepsy (Govindan et al., 2008; Kimiwada et al., 2006; Nilsson et al., 2008) by demonstrating that not only are these abnormalities evident in children with a relatively short duration of disorder, but that they can be seen near to the time of diagnosis of epilepsy, and occur in other epilepsy syndromes.

The corpus callosum has been previously implicated in adults with chronic temporal lobe epilepsy and to incur both DTI (Arfanakis et al., 2002; Kim et al., 2008; Thivard et al., 2005) and volumetric (Hermann et al., 2003b; Weber et al., 2007) abnormalities. In the present study the posterior corpus callosum exhibits reduced FA, increased D_{rad} and increased MD in epilepsy patients compared to controls. Interestingly, the finding of abnormal DTI took place in the absence of volumetric change in the same callosal region. This finding is in direct support of the idea that DTI is able to detect abnormalities not evident using conventional MRI techniques (Duncan, 2002). Other MRI studies have shown DTI abnormalities in the presence of volumetric differences (Gong et al., 2008), however to our knowledge this is the first study of epilepsy patients to exhibit a structure specific abnormality in diffusion but not volume.

Structural studies of the normal development of white matter in children suggest that the anterior corpus callosum matures before the mid or posterior regions (Giedd et al., 1999; Hasan et al., 2009). Our finding of DTI abnormality in the posterior but not anterior corpus callosum may indicate a preferential damage to later myelinating callosal regions. Furthermore, radial but not axial diffusivity was altered in the posterior corpus callosum. Although there is no

definitive microstructural change certain to underlie this pattern, there are a growing number of DTI studies relating altered D_{rad} to myelination abnormalities (Budde et al., 2007; Song et al., 2005) and showing a reduction of D_{rad} during normal white matter development in humans thought to correspond to compacting fibers and myelination (Alexander et al., 2007; Hasan et al., 2009; Snook et al., 2005). It is possible that the myelination of axons in the patients is slowed by the epileptogenic process or that there is seizure-related damage to the posterior corpus callosum myelin sheath surrounding the onset of epilepsy. In support of the view of myelin as a primary target, there is no observed group difference in gray matter volume in any lobar region to suggest axonal degeneration secondary to neuronal loss, although the limitations of volumetric measurements are recognized as specific layers of the neuropil may be affected but not detected by these volumetric measurements.

The other region that displays abnormal DTI values is the cingulum, in which FA is reduced and D_{rad} is increased. This finding is in agreement with several studies of chronic temporal lobe epilepsy populations (Concha et al., 2005; Concha et al., 2009; McDonald et al., 2008) and suggests a vulnerability of the cingulum that may accompany the onset of epilepsy. The internal capsule, external capsule and fornix were not significantly different from control values. It is possible that there is no change in these structures; however, they should not be ruled out of future studies without first addressing the limitations of this study.

Future studies will be needed to more fully characterize the structural state of the newly epileptic brain. This study provides an important initial characterization of DTI indices in this group, however there are several limitations that must be addressed. These include the small sample size and mixed epilepsy syndromes of the patient group and the imaging limitations of resolution and acquisition gap thickness, which was large and precluded the use of tractography or analysis of small white matter structures as well as measurement of complete white matter structures.

The finding of white matter vulnerability in this study is in conceptual agreement with previous MRI studies of patients with epilepsy. Diffuse abnormalities in cerebral white matter in focal epilepsy have been reported using both traditional volumetrics and voxel based morphometry (Hermann et al., 2003b; McMillan et al., 2004; Mueller et al., 2006; Seidenberg et al., 2005; Yu et al., 2008). Vulnerability of frontal-temporal connections including the uncinate and arcuate fasciculi have been described in temporal lobe epilepsy (Lin et al., 2008; Rodrigo et al., 2007) with verification of this abnormal connectivity and demonstration of their important linkages to well known cognitive abnormalities (Diehl et al., 2008; Flugel et al., 2006; Lui et al., 2005; McDonald et al., 2008; Powell et al., 2007; Yogarajah et al., 2008). Understanding the cause, course, and consequences of microstructural abnormalities of cerebral white matter should help to understand the etiology of neurobehavioral comorbidities of epilepsy.

Supplementary Material

Refer to Web version on PubMed Central for supplementary material.

Acknowledgments

The authors would like to thank the UW Institute for Clinical and Translational Research (ICTR) and support from the following sources: NIH RO144351, T90DK070079 and R90DK071515.

References

Alexander AL, Lee JE, Lazar M, Boudos R, DuBray MB, Oakes TR, Miller JN, Lu J, Jeong EK, McMahon WM, Bigler ED, Lainhart JE. Diffusion tensor imaging of the corpus callosum in Autism. *Neuroimage* 2007;34:61–73. [PubMed: 17023185]

- Andreasen NC, Rajarethinam R, Cizadlo T, Arndt S, Swayze VW 2nd, Flashman LA, O'Leary DS, Ehrhardt JC, Yuh WT. Automatic atlas-based volume estimation of human brain regions from MR images. *J Comput Assist Tomogr* 1996;20:98–106. [PubMed: 8576490]
- Arfanakis K, Hermann BP, Rogers BP, Carew JD, Seidenberg M, Meyerand ME. Diffusion tensor MRI in temporal lobe epilepsy. *Magn Reson Imaging* 2002;20:511–519. [PubMed: 12413596]
- Budde MD, Kim JH, Liang HF, Schmidt RE, Russell JH, Cross AH, Song SK. Toward accurate diagnosis of white matter pathology using diffusion tensor imaging. *Magn Reson Med* 2007;57:688–695. [PubMed: 17390365]
- Concha L, Beaulieu C, Gross DW. Bilateral limbic diffusion abnormalities in unilateral temporal lobe epilepsy. *Ann Neurol* 2005;57:188–196. [PubMed: 15562425]
- Concha L, Beaulieu C, Collins DL, Gross DW. White-matter diffusion abnormalities in temporal-lobe epilepsy with and without mesial temporal sclerosis. *J Neurol Neurosurg Psychiatry* 2009;80:312–319. [PubMed: 18977826]
- Deppe M, Kellinghaus C, Duning T, Moddel G, Mohammadi S, Deppe K, Schiffbauer H, Kugel H, Keller SS, Ringelstein EB, Knecht S. Nerve fiber impairment of anterior thalamocortical circuitry in juvenile myoclonic epilepsy. *Neurology* 2008;71:1981–1985. [PubMed: 19064879]
- Diehl B, Busch RM, Duncan JS, Piao Z, Tkach J, Luders HO. Abnormalities in diffusion tensor imaging of the uncinate fasciculus relate to reduced memory in temporal lobe epilepsy. *Epilepsia* 2008;49:1409–1418. [PubMed: 18397294]
- Duncan JS. Neuroimaging methods to evaluate the etiology and consequences of epilepsy. *Epilepsy Res* 2002;50:131–140. [PubMed: 12151124]
- Duncan JS. Imaging the Brain's Highways-Diffusion Tensor Imaging in Epilepsy. *Epilepsy Curr* 2008;8:85–89. [PubMed: 18596882]
- Flugel D, Cercignani M, Symms MR, O'Toole A, Thompson PJ, Koeppe MJ, Foong J. Diffusion tensor imaging findings and their correlation with neuropsychological deficits in patients with temporal lobe epilepsy and interictal psychosis. *Epilepsia* 2006;47:941–944. [PubMed: 16686662]
- Giedd JN, Blumenthal J, Jeffries NO, Rajapakse JC, Vaituzis AC, Liu H, Berry YC, Tobin M, Nelson J, Castellanos FX. Development of the human corpus callosum during childhood and adolescence: a longitudinal MRI study. *Prog Neuropsychopharmacol Biol Psychiatry* 1999;23:571–588. [PubMed: 10390717]
- Gong G, Concha L, Beaulieu C, Gross DW. Thalamic diffusion and volumetry in temporal lobe epilepsy with and without mesial temporal sclerosis. *Epilepsy Res* 2008;80:184–193. [PubMed: 18490143]
- Govindan RM, Makki MI, Sundaram SK, Juhasz C, Chugani HT. Diffusion tensor analysis of temporal and extra-temporal lobe tracts in temporal lobe epilepsy. *Epilepsy Res* 2008;80:30–41. [PubMed: 18436432]
- Gross DW, Concha L, Beaulieu C. Extratemporal white matter abnormalities in mesial temporal lobe epilepsy demonstrated with diffusion tensor imaging. *Epilepsia* 2006;47:1360–1363. [PubMed: 16922882]
- Harris G, Andreasen NC, Cizadlo T, Bailey JM, Bockholt HJ, Magnotta VA, Arndt S. Improving tissue classification in MRI: a three-dimensional multispectral discriminant analysis method with automated training class selection. *J Comput Assist Tomogr* 1999;23:144–154. [PubMed: 10050826]
- Hasan KM, Kamali A, Iftikhar A, Kramer LA, Papanicolaou AC, Fletcher JM, Ewing-Cobbs L. Diffusion tensor tractography quantification of the human corpus callosum fiber pathways across the lifespan. *Brain Res* 2009;1249:91–100. [PubMed: 18996095]
- Hermann B, Hansen R, Seidenberg M, Magnotta V, O'Leary D. Neurodevelopmental vulnerability of the corpus callosum to childhood onset localization-related epilepsy. *Neuroimage* 2003a;18:284–292. [PubMed: 12595183]
- Hermann B, Jones J, Sheth R, Dow C, Koehn M, Seidenberg M. Children with new-onset epilepsy: neuropsychological status and brain structure. *Brain* 2006;129:2609–2619. [PubMed: 16928696]
- Hermann BP, Seidenberg M, Bell B, Rutecki P, Sheth R, Sutula T, Wendt G, O'Leary D, Magnotta V. Extratemporal quantitative MRI volumetrics and neuropsychological function in temporal lobe epilepsy. *J Int Neuropsychol Soc* 2003b;9:353–362. [PubMed: 12666760]

- Kim H, Piao Z, Liu P, Bingaman W, Diehl B. Secondary white matter degeneration of the corpus callosum in patients with intractable temporal lobe epilepsy: a diffusion tensor imaging study. *Epilepsy Res* 2008;81:136–142. [PubMed: 18572387]
- Kimiwada T, Juhasz C, Makki M, Muzik O, Chugani DC, Asano E, Chugani HT. Hippocampal and thalamic diffusion abnormalities in children with temporal lobe epilepsy. *Epilepsia* 2006;47:167–175. [PubMed: 16417545]
- Lin JJ, Riley JD, Juranek J, Cramer SC. Vulnerability of the frontal-temporal connections in temporal lobe epilepsy. *Epilepsy Res* 2008;82:162–170. [PubMed: 18829258]
- Lui YW, Nusbaum AO, Barr WB, Johnson G, Babb JS, Orbach D, Kim A, Laliotis G, Devinsky O. Correlation of apparent diffusion coefficient with neuropsychological testing in temporal lobe epilepsy. *AJNR Am J Neuroradiol* 2005;26:1832–1839. [PubMed: 16091538]
- McDonald CR, Ahmadi ME, Hagler DJ, Tecoma ES, Iragui VJ, Gharapetian L, Dale AM, Halgren E. Diffusion tensor imaging correlates of memory and language impairments in temporal lobe epilepsy. *Neurology* 2008;71:1869–1876. [PubMed: 18946001]
- McMillan AB, Hermann BP, Johnson SC, Hansen RR, Seidenberg M, Meyerand ME. Voxel-based morphometry of unilateral temporal lobe epilepsy reveals abnormalities in cerebral white matter. *Neuroimage* 2004;23:167–174. [PubMed: 15325363]
- Mueller SG, Laxer KD, Cashdollar N, Buckley S, Paul C, Weiner MW. Voxel-based optimized morphometry (VBM) of gray and white matter in temporal lobe epilepsy (TLE) with and without mesial temporal sclerosis. *Epilepsia* 2006;47:900–907. [PubMed: 16686655]
- Nilsson D, Go C, Rutka JT, Rydenhag B, Mabbott DJ, Snead OC 3rd, Raybaud CR, Widjaja E. Bilateral diffusion tensor abnormalities of temporal lobe and cingulate gyrus white matter in children with temporal lobe epilepsy. *Epilepsy Res* 2008;81:128–135. [PubMed: 18595664]
- Powell HW, Parker GJ, Alexander DC, Symms MR, Boulby PA, Wheeler-Kingshott CA, Barker GJ, Koepp MJ, Duncan JS. Abnormalities of language networks in temporal lobe epilepsy. *Neuroimage* 2007;36:209–221. [PubMed: 17400477]
- Rodrigo S, Oppenheim C, Chassoux F, Golestani N, Cointepas Y, Poupon C, Semah F, Mangin JF, Le Bihan D, Meder JF. Uncinate fasciculus fiber tracking in mesial temporal lobe epilepsy. Initial findings. *Eur Radiol* 2007;17:1663–1668. [PubMed: 17219141]
- Seidenberg M, Kelly KG, Parrish J, Geary E, Dow C, Rutecki P, Hermann B. Ipsilateral and contralateral MRI volumetric abnormalities in chronic unilateral temporal lobe epilepsy and their clinical correlates. *Epilepsia* 2005;46:420–430. [PubMed: 15730540]
- Smith SM, Jenkinson M, Woolrich MW, Beckmann CF, Behrens TE, Johansen-Berg H, Bannister PR, De Luca M, Drobnjak I, Flitney DE, Niazy RK, Saunders J, Vickers J, Zhang Y, De Stefano N, Brady JM, Matthews PM. Advances in functional and structural MR image analysis and implementation as FSL. *Neuroimage* 2004;23:S208–219. [PubMed: 15501092]
- Snook L, Paulson LA, Roy D, Phillips L, Beaulieu C. Diffusion tensor imaging of neurodevelopment in children and young adults. *Neuroimage* 2005;26:1164–1173. [PubMed: 15961051]
- Song SK, Yoshino J, Le TQ, Lin SJ, Sun SW, Cross AH, Armstrong RC. Demyelination increases radial diffusivity in corpus callosum of mouse brain. *Neuroimage* 2005;26:132–140. [PubMed: 15862213]
- Thivard L, Lehericy S, Krainik A, Adam C, Dormont D, Chiras J, Baulac M, Dupont S. Diffusion tensor imaging in medial temporal lobe epilepsy with hippocampal sclerosis. *Neuroimage* 2005;28:682–690. [PubMed: 16084113]
- Weber B, Luders E, Faber J, Richter S, Quesada CM, Urbach H, Thompson PM, Toga AW, Elger CE, Helmstaedter C. Distinct regional atrophy in the corpus callosum of patients with temporal lobe epilepsy. *Brain* 2007;130:3149–3154. [PubMed: 17728360]
- Witelson SF. Hand and sex differences in the isthmus and genu of the human corpus callosum. A postmortem morphological study. *Brain* 1989;112(Pt 3):799–835. [PubMed: 2731030]
- Yogarajah M, Powell HW, Parker GJ, Alexander DC, Thompson PJ, Symms MR, Boulby P, Wheeler-Kingshott CA, Barker GJ, Koepp MJ, Duncan JS. Tractography of the parahippocampal gyrus and material specific memory impairment in unilateral temporal lobe epilepsy. *Neuroimage* 2008;40:1755–1764. [PubMed: 18314352]
- Yogarajah M, Duncan JS. Diffusion-based magnetic resonance imaging and tractography in epilepsy. *Epilepsia* 2008;49:189–200. [PubMed: 17941849]

Yu A, Li K, Li L, Shan B, Wang Y, Xue S. Whole-brain voxel-based morphometry of white matter in medial temporal lobe epilepsy. *Eur J Radiol* 2008;65:86–90. [PubMed: 17553646]

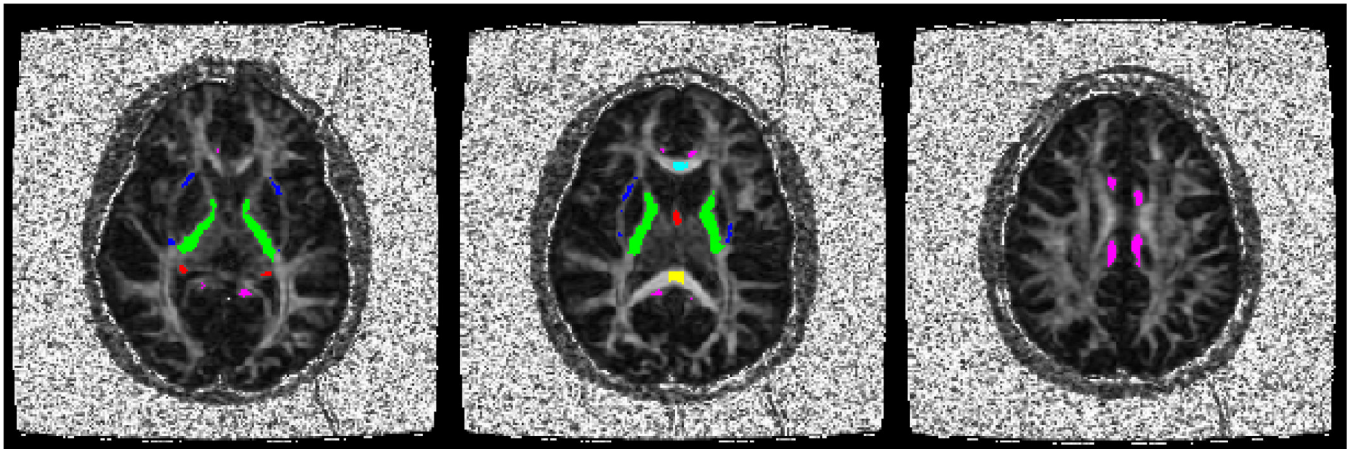


Figure 1.

Three axial slices from a representative FA map show image quality and ROI locations. Color coded ROIs are labeled as follows: cyan anterior corpus callosum, yellow - posterior corpus callosum, red - fornix, magenta - cingulum, green - internal capsule, blue - external capsule.

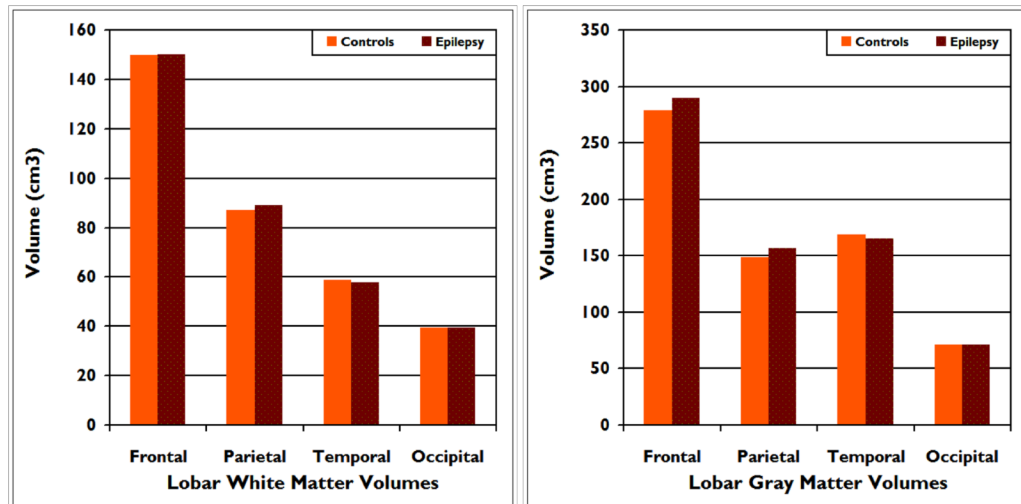


Figure 2. Mean total white (left panel) and gray (right panel) matter volumes for frontal, parietal, temporal and occipital lobes in children with epilepsy compared to healthy controls. There were no group differences across any of these regions of interest.

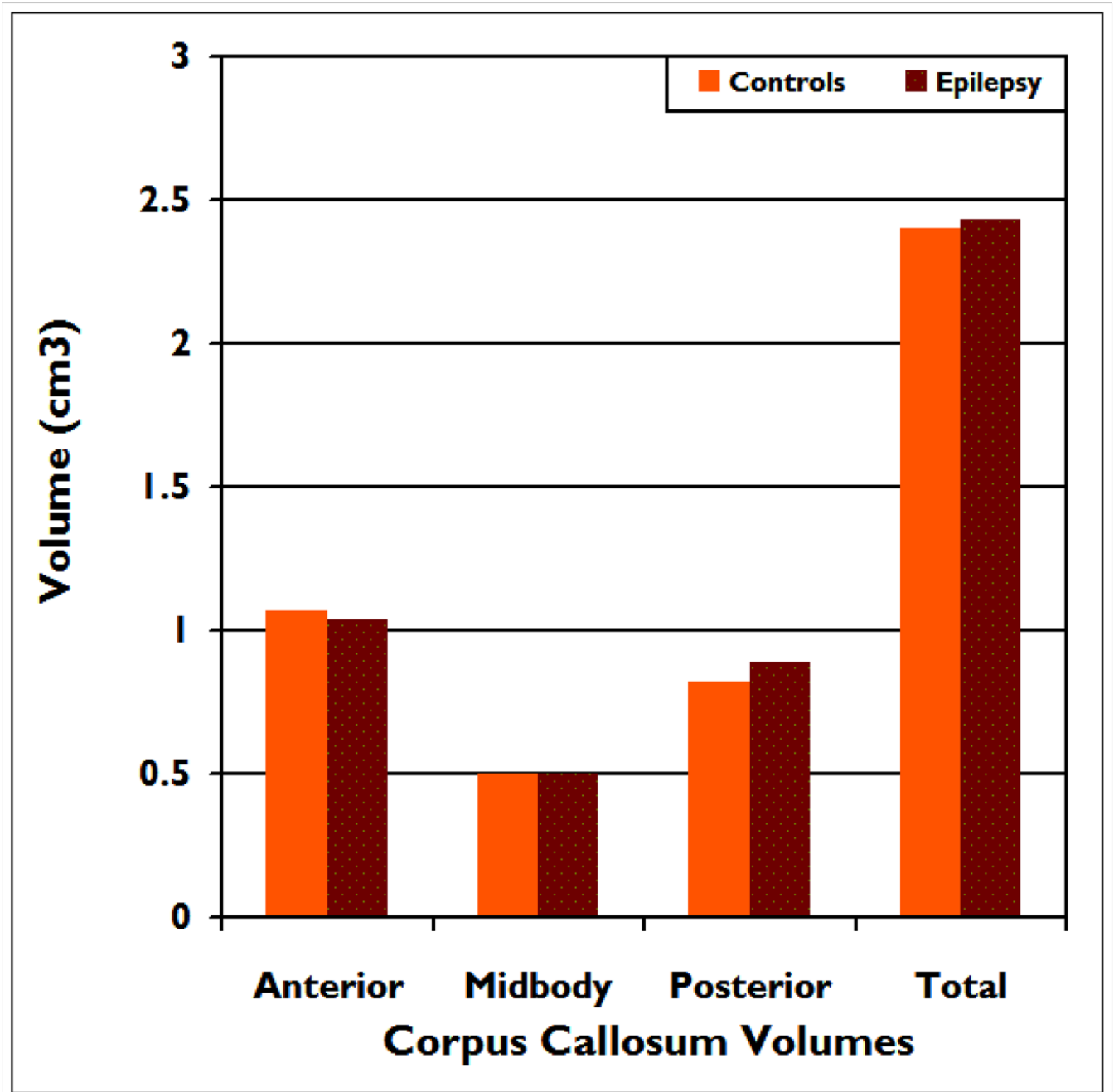


Figure 3. Mean volumes for anterior, midbody, posterior and total corpus callosum in children with epilepsy compared to healthy controls. There were no group differences across any of these regions of interest.

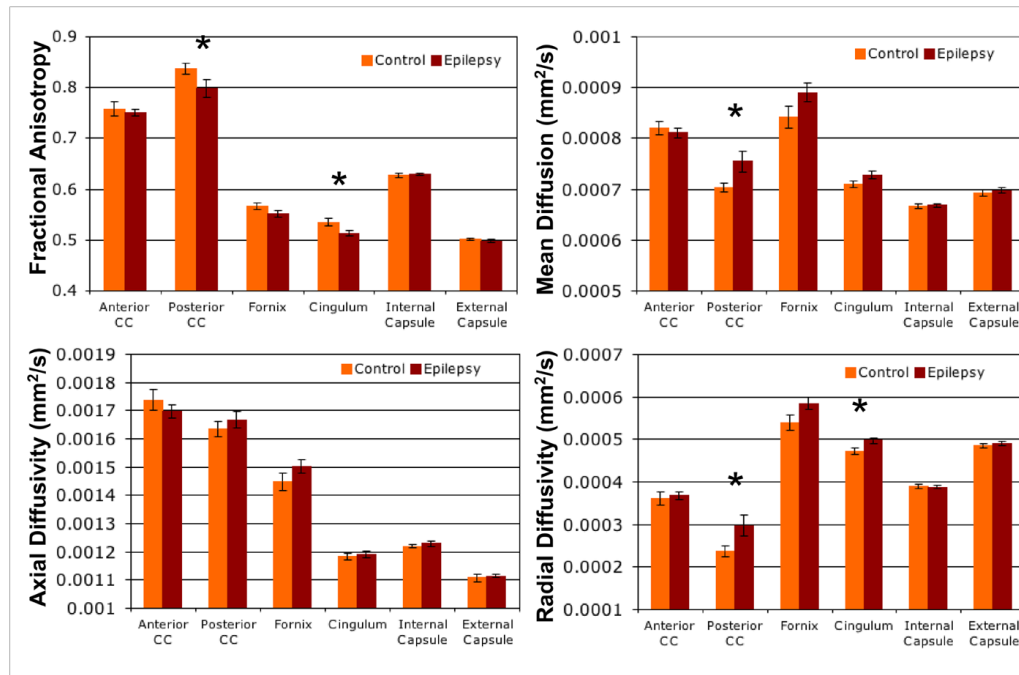


Figure 4. Mean DTI values (FA, MD, D_{ax} and D_{rad}) of six white matter structures (anterior and posterior corpus callosum, fornix, cingulum, internal capsule and external capsule) for epilepsy and control groups. * indicates $p < 0.05$ for group difference by analysis of covariance and error bars indicate standard error.

Table 1**Patient Syndrome information**

Syndrome distribution within the epilepsy patient group. Specific syndrome classifications within localization related and idiopathic generalized epilepsy groups are listed and the numbers of patients within each group are given.

Syndrome	number
Localization Related	11
Benign rolandic	4
Temporal Lobe	2
Frontal Lobe	1
Other Focal	4
Idiopathic Generalized	8
Juvenile absence	2
Juvenile myoclonic	5
Other Generalized	1